doi:10.26443/seismica.v4i1.1429

SEISMICA

Can Earthquake Locations Be Improved for Real-Time Monitoring? Revisiting the 1995 seismicity at Soufrière Hills Volcano, Montserrat

Jade H. W. Eyles * [1,2], **Jessica H. Johnson** [1], **Jenni Barclay** [3], **Paddy J. Smith** [4], **Victoria L. Miller** [5]

[1]School of Environmental Sciences, University of East Anglia, Norwich, UK, [2]Department of Earth, Atmospheric, and Planetary Sciences, Massachusetts Institute of Technology, Cambridge, USA, [3]School of Earth Sciences, University of Bristol, Bristol, UK, [4]School of Cosmic Physics, Dublin Institute for Advanced Studies, Dublin, Ireland, [5]GNS Science, Lower Hutt, NZ

Author contributions: *Conceptualization*: Jade H. W. Eyles, Jessica H. Johnson, Jenni Barclay, Paddy J. Smith, Victoria L. Miller. *Formal Analysis*: Jade H. W. Eyles, Jessica H. Johnson, Jenni Barclay, Paddy J. Smith, Victoria L. Miller. *Writing - Original draft*: Jade H. W. Eyles. *Writing - Review & Editing*: Jessica H. Johnson, Jenni Barclay, Paddy J. Smith, Victoria L. Miller.

Abstract Volcanic earthquakes provide a wealth of information about the magmatic system. Monitoring volcanic seismicity is one of the primary methods used by volcano observatories globally, including at Soufrière Hills Volcano, Montserrat. Computed earthquake locations represent the optimal solution given the information available and vary depending on the chosen location method and seismic velocity model, but rarely are these parameters tested for suitability in each region. We propose a new method that utilises synthetic earthquakes to evaluate whether the calculated hypocenters and their associated errors accurately represent the true source locations. We define this evaluation as a confidence parameter that highlights events we can 'trust'. By comparing several location methods and seismic velocity models for Montserrat we show the current setup is not optimal and suggest an alternative location method. Analysis using new 'trusted' relocations focuses on four seismic clusters distal from Soufrière Hills in 1995. Our results highlight differences in hypocenters during this period, suggesting alternative interpretations of the distal seismicity. We propose a WNW dyke orientation, supporting previous studies, and local fault complexes in the region. Overall, this paper highlights the importance of using a robust location method suitable for the region to ensure that calculated hypocenters are trustworthy and accurate. Use of sub-optimal methods can influence apparent spatial earthquake trends, impacting interpretations and our understanding of volcanic systems.

Production Editor:
Andrea Llenos
Handling Editor:
Stephen Hicks
Copy & Layout Editor:
Ethan Williams

Received:
20 August 2024
Accepted:
31 March 2025
Published:
1 May 2025

1 Introduction

Volcanic seismicity is one of the main indicators used by observatories to monitor the activity of volcanoes worldwide. The number of events, the type of the seismic signal and the distribution of hypocenters can all give information about the internal dynamics of the volcanic system. Accurate earthquake locations can greatly improve the understanding of subsurface processes at volcanoes globally. The quality of the calculated hypocenter depends on the location method used (combination of arrival time picks and associated pick error, velocity model, travel time uncertainties and location algorithm), resulting in varied output locations when computed by different users. However, location methods are not always tested for suitability in each region, reducing our understanding of how accurately these perform, and if calculated hypocenters could be improved. Testing of location methods is essential for constraining hypocenters and can be used to unravel more information from existing data before deploying further networks.

Volcanic observatories use a range of softwares and methodologies for earthquake location. A software package frequently used for earthquake detection is Earthworm—this has several built in programs that are able to collect, process and analyse the data (Johnson et al., 1995). The USGS observatories (HVO, CVO, AVO) commonly use the location package Hypoinverse (Klein, 2002) for preliminary earthquake locations, which are then refined using joint relocation methods such as HypoDD (Waldhauser, 2001). GeoNet in New Zealand uses a mixture of LocSAT (Bratt and Nagy, 1991) and NonLinLoc (Lomax, 2001) for earthquake location, whereas INGV uses the program Caravel (built on Earthworm, Bono et al. (2021)), for their initial manual locations which are then refined by the on-duty seismologists.

Synthetic earthquakes (where the location of the earthquake is controlled and corresponding travel times to seismic stations are calculated) eliminates the unknown of the original earthquake hypocenter (for X, Y, Z, t parameters), allowing the velocity model and location algorithm to be tested for suitability in each region. We present a new method where synthetic earthquakes are used to determine how trustworthy the calculated hypocenters are, and how this can be used alongside other parameters to understand which

*Corresponding author: jeyles95@mit.edu

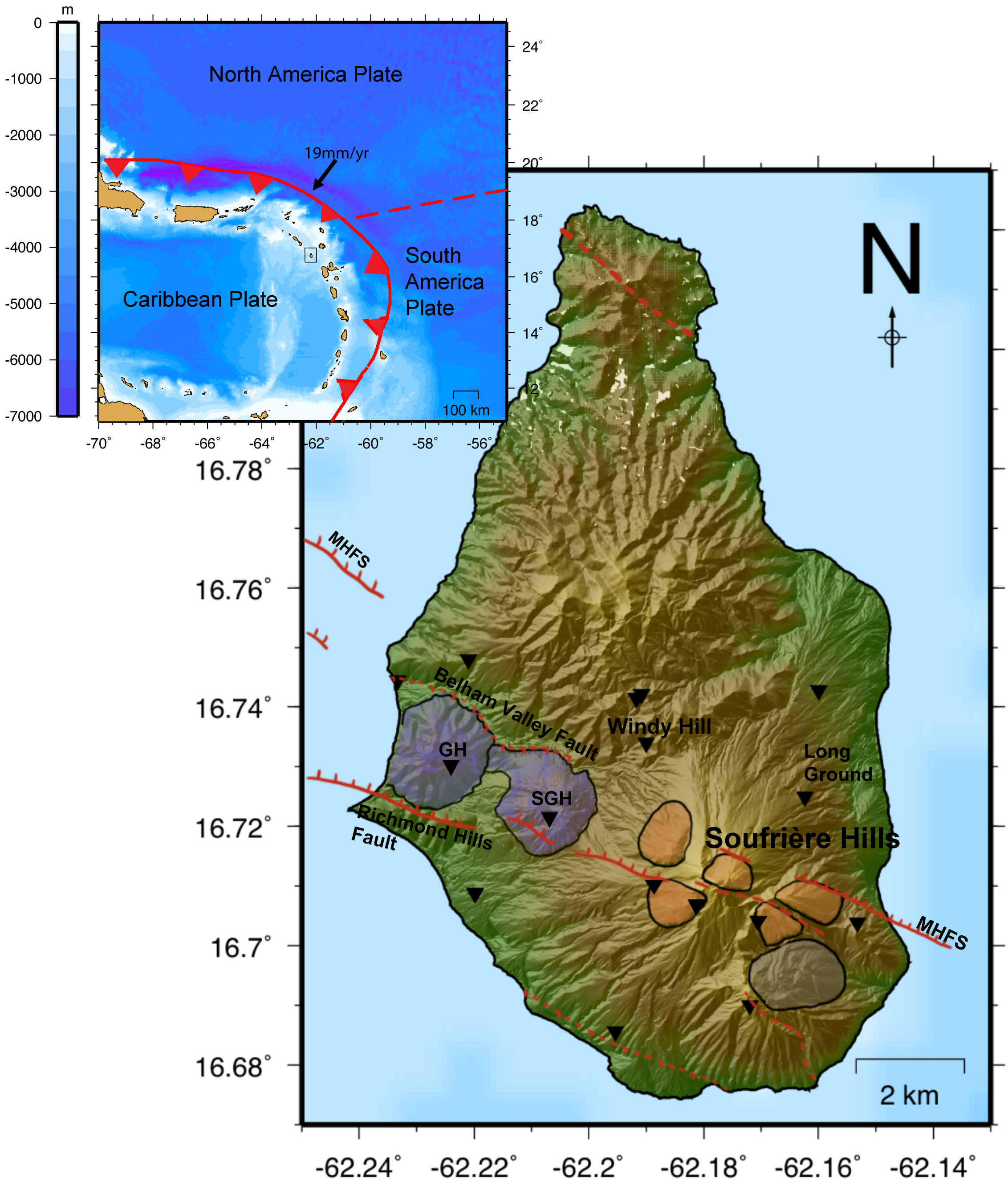

Figure 1 Map of the island of Montserrat showing main landmarks and geological features adapted from Baird et al. (2015). Coloured regions represent volcanic complexes grouped by age; grey: South Soufrière dome, orange: complexes of Soufrière Hills (170 ka to present), purple: Garibaldi Hill and St Georges Hill complex (282 ka). Annotations: GH = Garibaldi Hill, SGH = St George's Hill, MHFS = Montserrat-Havers Fault System. Red lines represent main faults in the region. Inverted triangles represent seismic network from July–November 1995. Inset shows the location of Montserrat in the Lesser Antilles. Red line denotes plate boundaries between the North America, South American and Caribbean plate. Plate boundaries taken from Bird (2003). Arrows show plate motions.

methods and models are most suitable for each region. This provides a simple analysis to improve earthquake hypocenters that can benefit observatories with time and computational constraints. Our proposed method can be tailored for inclusion of other criteria such as pick quality and station corrections and easily adapted for testing in other volcanic and seismically active regions to improve past and future seismic catalogues. It is worth noting that the use of station corrections in volcanic settings is not always suitable due to the constantly changing subsurface structure during periods of unrest. Additional techniques such as joint location methods have been shown to greatly improve earthquake hypocenters and minimise errors, and additionally remove the need for station corrections (Richards and W-Y, 2006). These techniques are rarely used for real-time monitoring, and therefore we focus purely on improving initial absolute locations that are frequently used by observatories for hazard assessment.

Montserrat is a small volcanic island situated in the Lesser Antilles, north-west of Guadeloupe (Figure 1). Soufrière Hills Volcano is situated in the south of the island and began erupting in July 1995 after three years of increased seismicity (Young et al., 1998). It has undergone five main phases of extrusion with the last recorded extrusion in 2010; monitoring data still shows signs of unrest at the time of writing (MVO, 2023). The Montserrat Volcano Observatory (MVO) uses seismic analysis as one of its primary monitoring tools; however, the method used to derive locations has not been updated since the broadband network was installed in October 1996. Currently, MVO uses the location method Hypocenter (Lienert et al., 1986) with a simple 1D velocity model of Montserrat that was adapted from a velocity model of Guadeloupe. MVO's seismic catalogue from July 1995 to February 2018 contains over 13,000 located events. This catalogue provides a great wealth of information throughout the course of the eruption that allows changes in seismicity to be linked to volcanic processes as the system stabilised. Understanding weaknesses associated with current hypocenters, and how uncertainties in these locations can be improved, can provide a new insight into the volcanic system.

Our new method is applied to seismicity in Montserrat for the purpose of assessing how seismic monitoring and location procedures could be updated, and whether improved hypocenters can assist in elucidating the crustal-magmatic system of Soufrière Hills volcano. We tested MVO's station configuration as of February 2020 with a range of location algorithms and velocity models to understand which location setup is optimal for locating earthquakes on Montserrat. This optimal method was used to relocate MVO's past seismic catalogue for all event types. An example of the importance of improved hypocenters is shown for four clusters distal to the main seismicity beneath Soufrière Hills that were recorded during July–November 1995 at the start of the eruption. Several distal clusters have been observed by Aspinall et al. (1998), Miller et al. (2010) and White and McCausland (2016) throughout 1995 with conflicting interpretations. Our new 'trusted' hypocenters are used to shed light on the implications of using poorly constrained hypocenters for initial earthquake locations, and how this alters our interpretations of the volcanic system during this time period.

2 Methods

The true earthquake location is never known, with the calculated hypocenter being an optimal solution given the travel times and models provided. Calculated hypocenters vary when using different location algorithms and velocity models. Therefore, it is important that the methodology is tested and compared with alternative methods to understand how trustworthy the calculated hypocenters are. This type of method testing can be applied to any volcanic region, with the parameters and models optimised to suit each region. We focussed on improving calculated earthquake hypocenters at Montserrat during the course of the eruption from 1995–2018, with a direct focus on relocations in 1995 where several distal clusters were observed. It is important to understand if new advances in location algorithms and alternative seismic velocity models can improve initial hypocenters for existing seismic data, refining previous interpretations of the volcanic system.

We produced a 15 by 20 km grid of synthetic earthquakes spaced at 1 km (Figure S1); this was created at depths of 0.5 km above sea level, 0, 1, 3, 5, 5.8 and 10 km below sea level (bsl) to ensure that the velocity model for Montserrat was adequately sampled. A depth of 5.8 km was used to test the limits of one velocity model which only extended to a depth of 6 km. Synthetic P and S wave arrival times were calculated from each synthetic point to all active seismic stations using each tested velocity model (resulting in multiple sets of arrival times for each velocity model setup). Topography was not included in this calculation. Synthetic arrival times were calculated using the eikonal finite-difference scheme of Podvin and Lecomte (1991). This uses a systematic application of Huygens principle with finite difference approximation and takes into account varying propagation modes and local discontinuities when calculating travel times (Podvin and Lecomte, 1991). This resulted in a set of arrival times that could be used to locate the synthetic earthquake with each location method that was being tested, defined as the synthetic hypocenter. NonLinLoc uses this method to calculate travel time grids, whereas with the program Hypocenter, the user either uploads their own travel time grid or can calculate this using a program called TTGEN.

The number of seismic stations on Montserrat has varied over the past 25 years with the network being continuously revised and updated, with some stations being destroyed during the 1995 eruption. The seismic stations used for creating synthetic travel times are shown in Figure S2, and represent MVO stations that were active in February 2020; details of the seismic stations used are shown in Table S1. This configuration was used to improve MVO's current location method for future earthquakes located on Montserrat. We tested 10 different seismic station configurations that were available from 1995 to February 2020 and found all configurations with more than four seismic stations produced similar hypocenter errors and changes in location, allowing results from this synthetic test to be suitable for relocation of all MVO events from 1995. An example of changes in location for each of the station configurations tested are shown in Figure S3. Station corrections were not included with synthetic testing to align with MVO's earthquake location procedures, as our goal was

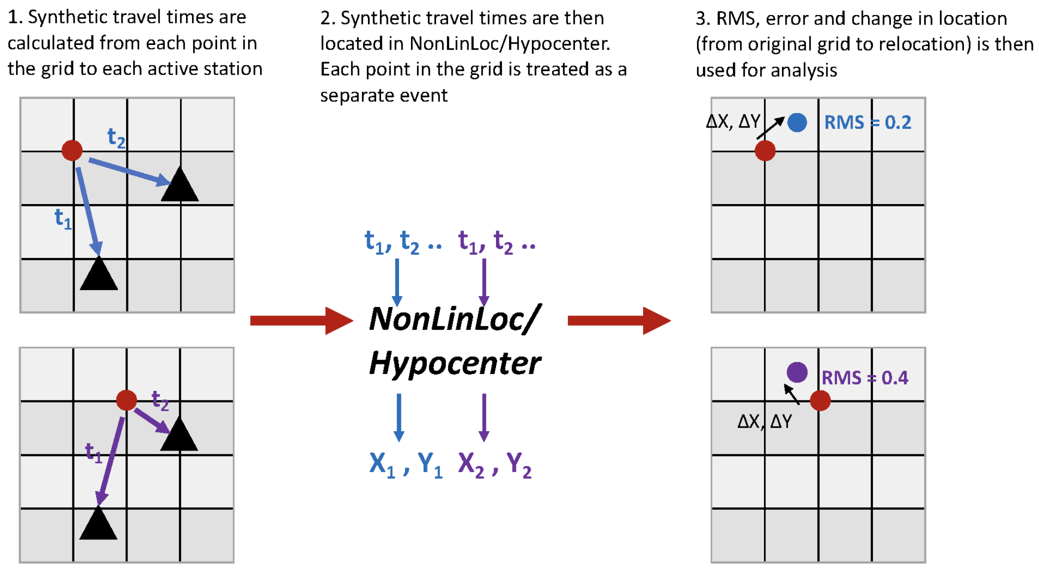

Figure 2 A simplified 2D schematic explaining the methodology used to relocate the synthetic earthquakes; in our testing this was also done for depth locations. The red dot represents the synthetic grid location, with the blue and purple dot representing the calculated hypocenter. t_1 and t_2 are travel times from each station, and X_1, Y_1, and X_2, Y_2 are the relocated locations for each synthetic earthquake.

to maintain consistency with current and future operations.

To understand how well the synthetic earthquakes were being located, the parameter 'trusted' was created to show how reliable the calculated hypocenters were. The 'trusted' parameter is binary, and uses the distance of the calculated hypocenter from the original synthetic location to determine whether this distance is within the calculated error of the synthetic hypocenter. A trusted event is an earthquake that has the original synthetic location within the computed error of the calculated hypocenter—i.e. the 68% confidence ellipsoid covers the original synthetic location. This was computed for the X, Y and Z location individually, with each relocated synthetic event being labelled as trusted or untrusted. The computed error used is the covariance calculated by each location method and then converted into a standard error (X, Y and Z) using the equations taken from Lomax (2001) so that each method can be compared equally. An untrusted location is a hypocenter that is located further away from the original synthetic location than the calculated error.

The synthetic arrival times were calculated using a gaussian error of 0.1 seconds, representing a high quality arrival time, and assumes that all seismic stations were fully operational. This was deemed suitable due to MVO handpicking P and S wave arrival times, although we note that MVO's pick errors could be larger during the early stages of the eruption when a greater number of analysts were picking events. A range of errors were tested for calculating the synthetic arrival times, varying from 0.1 to 5 seconds to understand the impact on calculated hypocenter error (Figure S4). This variation in error for calculating the arrival time represents the pick error when events are handpicked by an analyst. Higher pick error increases hypocenter uncertainty and results in a decrease in the number of trusted earthquakes.

Differences in location between the synthetic and calculated hypocenter were compared with the RMS of the calculated origin time, calculated hypocenter error, and the number of trusted earthquakes. A schematic of this procedure is shown in Figure 2. Comparing calculated errors, and changes in location between synthetic and calculated earthquakes alone can not provide a concrete understanding of which location setups perform best. The trusted parameter provides an important way of quantitatively comparing each location method, to aid understanding of which setup provides realistic hypocentral information. Some methods may produce lower calculated hypocenter errors, but, if these are not consistent with changes in location, then the setup could be under-calculating the error. The trusted parameter takes both elements into account, providing a parameter that describes if the location setup is representative of the output hypocenter. Using this in conjunction with changes in location and calculated error, provides a strong indication of which setups are reliable for earthquake location on Montserrat. Finally, a Dunn's statistical analysis compared all relocations of synthetic events to check if there was a significant reduction in calculated errors and change in location between each tested setup.

2.1 Velocity Models

Three alternative velocity models to the MVO seismic velocity model were tested for comparison of suitability in this study; this resulted in three 1D models (Figure S5) and one 3D model. The MVO model comprises five layers, and was adapted with trial and error modifications from a starting model based on Guadeloupe

Table 1 Labels and descriptions of each velocity model and location method used for comparison in earthquake location.

Velocity Models		Location Algorithms	
V1	MVO (Power et al., 1998)	**Method 1**	*Hypocenter* (Lienert et al., 1986)
V2	Rowe et al. (2004)	**Method 2**	*NonLinLoc* using the Gaussian Inversion (Lomax, 2001)
V3	1D SEA-CALIPSO (Shalev et al. (2010))	**Method 3**	*NonLinLoc* using the Equal Differential Time method (Lomax, 2001)
V4	3D SEA-CALIPSO (Paulatto et al. (2012))	**Method 4**	*NonLinLoc* using the Gaussian Inversion and equally weighted arrival times (Lomax, 2001)

(Power et al., 1998). The 1D Rowe et al. (2004) model was produced with the tomography program VELEST and Simul2000 using arrival times of shallow seismicity from 1995–1996. The 1D SEA-CALIPSO model was adapted by Miller (2011) using a 3D model by Shalev et al. (2010); this was determined by P wave first arrivals at 58 seismic stations on land and sea during the SEA-CALIPSO project. The 3D seismic velocity model from Paulatto et al. (2012) was generated using a mixture of ocean and land seismometers during the active source SEA-CALIPSO project and inverted using the tomography code of Hobro et al. (2003). These models were chosen due to them being publicly available, and therefore would be the models tested if MVO were to follow the methodology outlined in this paper without the computation of creating a new 1D seismic velocity model.

2.2 Location Algorithms

Two location programs were used for this study: *Hypocenter* (Lienert et al., 1986), which is currently used by MVO, and *NonLinLoc* (Lomax, 2001), which has been proven to work well in complex environments. *Hypocenter* follows Geiger's method, which uses a centred and scaled, linearised least squares approach with adaptive damping to solve earthquake location and origin time (Lienert et al., 1986). *NonLinLoc* uses a direct search method that determines a 3D spatial probability density function (PDF) over a given region for all possible solutions. This provides a grid of PDF values, with the optimal solution taken as the maximum value of the PDF.

Current MVO settings and parameters were used with the location method *Hypocenter*; this was to keep it consistent when comparing different velocity models and location methods to present day MVO locations. A 3D model cannot be input into *Hypocenter*, and therefore this was only tested with three 1D seismic velocity models. The Oct-Tree sampling method was chosen as the search method for *NonLinLoc* with three variations of location algorithms tested. This included: the Equal Differential Time (EDT) method, the Gaussian Analytical (GAU) method, and the Gaussian Analytical methods with all arrival times equally weighted.

2.3 Tested Setups

We tested four velocity models and four location methods shown in Table 1 (including the traditional velocity model and method employed by MVO, referred to as the 'MVO setup'). This resulted in 15 different location setups tested with the synthetic earthquake grids (due to *Hypocenter* not allowing the input of 3D seismic velocity models).

3 Results

Parameters including RMS of calculated origin time, calculated hypocenter errors, changes in location between synthetic and original hypocenters, and the percentage of trusted hypocenters were used to determine which setup was optimal for locating earthquakes on the island of Montserrat. Figure 3 shows the percentage of trusted earthquakes for each combination of method and velocity model. The full trust table can be found in Figure S6. The MVO setup (method 1 and V1) performed well at shallow depths, but had larger calculated errors and was not as trustworthy for Z (depth) estimates. Method 3 performed well for all velocity models and depths on average compared to other tested methods.

Changes in location and calculated errors for each setup can be found in Figure S7 and S8 respectively; these results were also used in combination with the trust table to determine the optimal location method. The MVO setup consistently underperformed, and all velocity models used with method 1 showed higher RMS, change in location and errors compared to other location methods. This can be clearly seen in Figure S9, which visualises the change in location for each setup when the synthetic earthquakes are set at 0 km depth. Methods 2 and 3 produced the lowest changes in locations for X, Y and Z constraints, suggesting a more accurate hypocenter had been calculated. Methods 2 and 4 produced consistently lower hypocenter errors than method 3. This was to be expected as method 3's algorithm takes into account outliers when generating the PDF, resulting in hypocenters with more representative errors, which are generally larger.

		Method 1			Method 2				Method 3				Method 4			
		V1	V2	V3	V1	V2	V3	V4	V1	V2	V3	V4	V1	V2	V3	V4
0 km	x	83.6	11.0	37.2	83.6	83.6	82.4	66.7	87.5	89.9	89.3	88.1	82.1	82.1	81.5	66.7
	y	95.5	14.6	45.8	80.7	81.3	75.9	61.0	85.7	86.6	81.8	86.9	80.4	80.1	75.6	61.3
	z	39.0	18.5	10.4	70.2	72.9	78.0	17.0	77.7	78.6	83.9	93.8	68.8	1.5	78.3	17.0
1 km	x	78.9	11.6	28.0	81.3	82.4	79.5	65.5	86.9	90.8	88.1	91.7	79.8	81.5	77.4	64.6
	y	90.5	10.7	32.1	73.8	82.7	78.6	58.6	80.4	87.5	81.5	89.0	72.9	81.8	77.7	58.6
	z	25.6	14.6	10.1	77.1	84.8	73.5	11.3	84.2	89.9	80.1	86.0	76.8	84.8	74.1	10.7
5 km	x	73.5	13.4	16.4	77.4	77.4	84.8	25.9	83.3	82.4	89.0	88.4	76.2	76.5	83.6	25.6
	y	58.3	5.4	17.6	75.3	70.5	83.9	15.5	79.5	75.9	89.0	88.1	75.3	68.8	83.6	15.2
	z	63.1	21.1	62.8	55.1	48.2	75.6	38.7	57.7	50.9	84.5	78.9	56.0	47.9	75.9	37.8
10km	x	95.24	16.96	X	83.33	85.42	X	22.32	89.58	88.69	X	89.88	81.85	84.52	X	22.32
	y	71.73	1.49	X	84.23	85.71	X	7.74	88.99	91.67	X	89.29	84.82	85.71	X	7.44
	z	84.23	6.55	X	86.90	86.90	X	94.05	95.54	95.54	X	93.45	86.61	85.71	X	93.75

> 90%
> 85%
> 80%
> 70%
> 60%
Optimal Method

Figure 3 Figure shows the percentage of trusted hypocenters for the X, Y, Z location, for each velocity model and location method. V1: MVO velocity model, V2: Rowe et al. (2004) velocity model, V3: 1D SEA-CALIPSO model by Shalev and Lees (1998); V4: 3D SEA-CALIPSO model by Paulatto et al. (2012). Method 1: *Hypocenter* with settings used by MVO, Method 2: *NonLinLoc* with the Gaussian Inversion, Method 3: *NonLinLoc* with the EDT method, Method 4: *NonLinLoc* with the Gaussian Inversion and equally weighted stations. Orange shows percentages higher than 60%, yellow higher than 70%, light green higher than 80% and dark green higher than 85%. The red outlined cells show the best velocity model/location method for that depth.

V2 performed best at depths of 0, 1 and 3 km, with V3 performing better at depths of 5 km. However, V3 was limited to a depth of 6 km due to the cut off of the generated velocity model. V2 performed well at additional depths up to 10 km with changes in location of 200–300 m compared to V3 at 5 km depth (Figure S7). Therefore V2 was more practical for relocating earthquakes on Montserrat, given a) its ability to locate deeper events which may be indicators of future unrest episodes, and b) producing significantly smaller changes in locations and errors compared to other models at shallower depths, where the majority of seismicity is currently located on Montserrat. Little difference in hypocenter errors was seen between methods 2, 3 and 4 when using V2, but method 3 produced a greater number of trusted earthquakes (Figure S8). It is more important to have a greater number of trusted earthquakes, especially when the difference in errors is minimal, as this gives us greater confidence in our interpretations.

A Dunn statistical test (Dunn, 1964) was performed for each combination of location method and velocity model to check that the results for each relocation were significantly different to each other, and hence the new location setup would produce a significant difference in calculated hypocenters. This tests between each pair of relocations to calculate the probability of observing a randomly selected value from the first group that is larger than a randomly selected value from the second group. The Dunn test was used with the Berronni method and adjusted p-values, which was computed in *R*, and tested between each pair of the 15 relocations. This was performed on both changes in location and hypocenter error at each depth of the synthetic data; the results for the statistical tests for change in location and error are shown in Figures S10 and S11 respectively. The results showed that V3 had significantly lower changes in X and Y locations at depths greater than 5 km compared to other velocity models, but that V2 had significantly lower changes in location at depths shallower than 3 km, supporting previous results. Overall, method 3 with V2 produced significantly lower changes in location and hypocenter errors than the current MVO setup. This supported results from the error tests and confirmed this method setup is optimal for locating earthquakes on Montserrat.

Method 3 with V2 was deemed the optimal setup as it performed well at all depths, with a high percentage of trusted earthquakes and small calculated hypocenter errors. This setup used the location method *NonLinLoc* with the EDT search method, alongside the seismic velocity model proposed by Rowe et al. (2004). This optimal setup was used to relocate the seismic catalogue on Montserrat for all available earthquakes in MVO's catalogue from 1995–2018. For demonstration, we have examined a subset of these data from July–November 1995 where a large amount of earthquakes were recorded distal (greater than 3 km) to Soufrière Hills.

4 Discussion

The MVO seismic catalogue from July 1995 to February 2018 was relocated using the Rowe et al. (2004) velocity model with the NonLinLoc EDT location method. MVO's arrival picks were weighted by pick quality and include both P and S wave arrivals; these were picked by several analysts throughout the eruption and may be inconsistent between time periods resulting in larger pick errors. Station corrections were not included in relocation due to MVO not currently using these for earthquake location and to make a fair comparison between

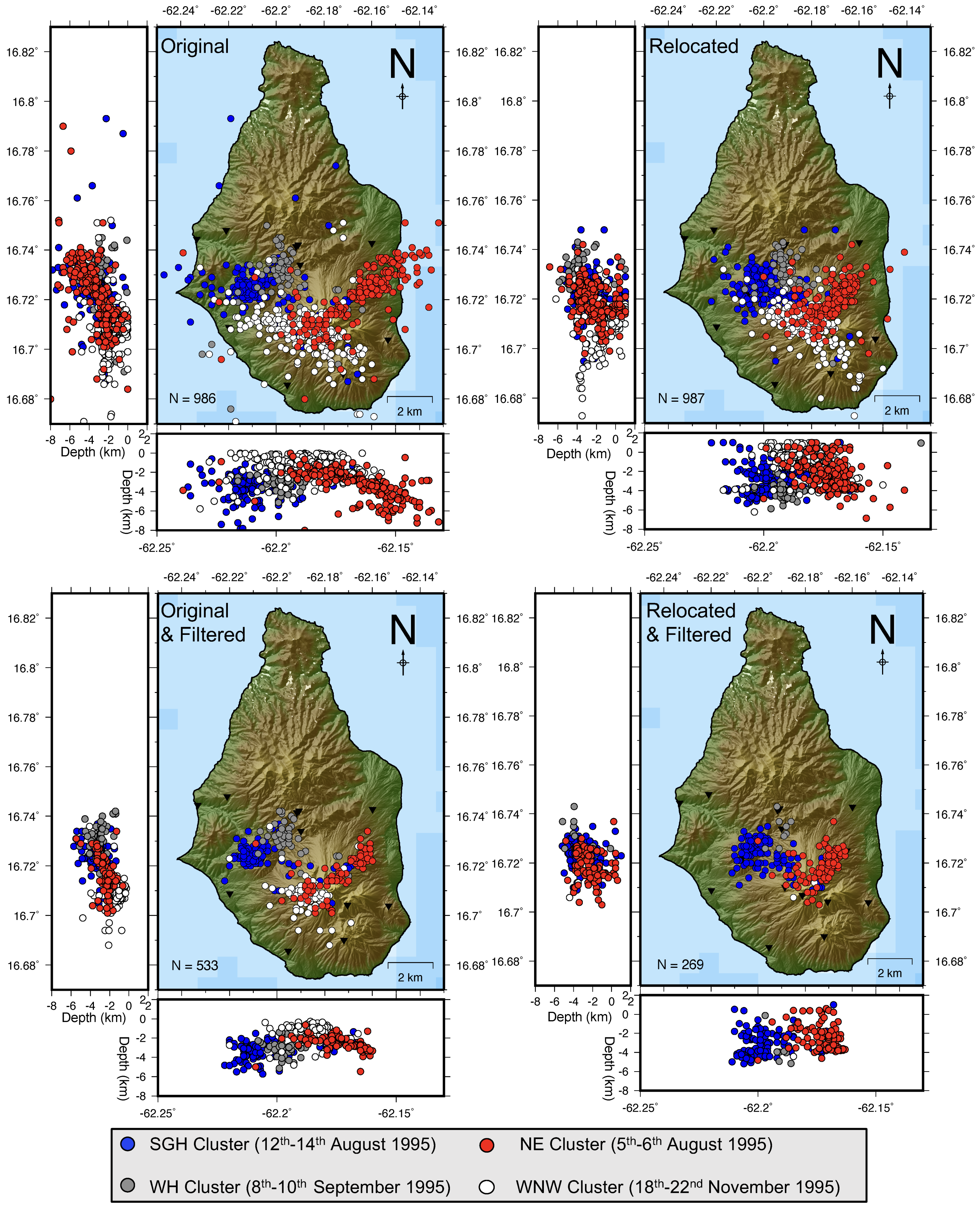

Figure 4 Original MVO setup hypocenters and our optimal setup hypocenters for four distal clusters from July–November 1995. Depth plots are shown with 0 representing sea level surface. The top panels shows all located earthquakes; bottom panels shows earthquakes which have been filtered for hypocentral errors less than 3 km, azimuthal gap $< 180°$, and RMS less than 0.2 seconds. Inverted triangles represent seismic stations active during 1995. WH = Windy Hill; SGH = St Georges Hill.

the two location setups.

Our aim was to improve earthquake hypocenters in real-time operations by volcanic observatories, where repicking of arrival times over longer timescales is not possible. Therefore, we used analysts' picks from MVO to replicate how the observatory would locate their seismicity during unrest. Data is often repicked in hindsight, which can improve pick and location quality. Alternative arrival times are available from Roman et al. (2008), who repicked P and S wave arrivals for all volcano-tectonic earthquakes from 1995–2007, improving the accuracy of calculated earthquake hypocenters. To test the difference in our hypocenters and understand how repicked waveforms would impact our locations, we used the arrival time picks from Roman et al. (2008) for relocation for the period of July–December 1995 using our optimal location setup. We found a similar distribution in hypocenter error between both datasets shown in Figure S12, with a slight improvement in RMS for Roman et al. (2008) locations of on average around 0.1 seconds. This suggests that Roman et al. (2008) locations are more reliable, which is to be expected given that these were repicked and therefore represent a high pick quality. However, there were almost four times the number of earthquakes constrained when using the MVO picks. Using Figure S4, we can see that if we increase the pick error from 0.1 to 1 second (likely for the MVO picks) we have a reduction of 10% in trusted events. However, given the increase in the number of events, this still provides an overall benefit to use for location, with the note that some events may be less trustworthy. Additionally, locations using Roman et al. (2008) picks showed similar hypocenters to using MVO picks. Therefore, we are confident in using MVO's arrival picks for interpretation of the dataset, replicating how an observatory would operate in real-time.

We focused on seismicity recorded between July and December 1995, coincident with the opening phase of the volcanic eruption. Seismic stations active during this time frame are shown in Figure S13 and Table S2, with the final earthquake catalogue for this time period shown in Table S3. Several features within the seismic catalogue for the beginning of the eruption in 1995 have been used as evidence for interpretations and models of dynamics of Soufrière Hills Volcano and magma plumbing geometry. Synthetic testing has shown that calculated hypocenters rely heavily on the method and velocity model used. Therefore, the calculated hypocenters may not be 'trusted' and many features of the catalogue may not be robust. This time period is particularly interesting due to several distal seismic clusters that were recorded. These distal clusters have been previously investigated by Aspinall et al. (1998) and Miller et al. (2010), but each investigation yielded different results and hence interpretations. MVO hypocenters were taken from Aspinall et al. (1998) during July 1995–October 1996; these events generally have higher errors associated with them compared to later time periods.

Four main distal clusters were highlighted during July–December 1995, resulting in a subset of 985 earthquakes that were further analysed from our relocations: beneath St George's Hill (SGH) from 11 to 14 August; from Soufrière Hills towards Long Ground (referred to as the NE cluster) from 5 to 6 August; beneath Windy Hill (WH) from 8 to 10 September; and a WNW trend in seismicity from 18 to 22 November (referred to as the WNW cluster). Relocated hypocenters are filtered for horizontal and depth errors less than 3 km, azimuthal gap $< 180°$, and RMS less than 0.2 seconds, resulting in 269 high-quality hypocenters used for further analysis. Both the WH and WNW cluster had less than 10 earthquakes once filtered for quality, resulting in only the SGH and NE cluster being studied further. Figure 4 displays the comparison of hypocenters determined using the MVO setup and our relocations using the chosen optimal setup for both filtered and unfiltered hypocenters. The MVO setup does produce a greater number of hypocenters when filtered for events less than 3 km, but synthetic testing has proven these to be less trustworthy. The MVO setup shows a more defined structure, especially in the NE cluster which shows an increase in depth towards the NE, which is not as clearly seen with the optimal setup. We believe this to be an artefact due to also seeing this trend in other time periods at Montserrat when using the MVO setup and for events with a small number of arrival time picks. Events that were filtered for the optimal setup generally had less than eight arrival times used for hypocenter calculation, increasing the location error, whereas the MVO setup was less affected by the low number of arrival picks producing low errors that have been shown to not be representative of the true error from our synthetic testing.

Hypocenters calculated using the optimal setup show several distinct differences to those from the MVO setup, with clusters being more confined and not extending as great a distance from Soufrière Hills. The WH cluster shows the greatest similarity in locations, with hypocenters located just to the west of St George's Hill. The WNW cluster is now centered more to the NW and closer to St George's Hill. Both the WH and WNW cluster do not show this pattern once we filter hypocenters to include only high quality events. The SGH cluster shows a significant change in location, with hypocenters connecting the western flanks of Soufrière Hills Volcano and St George's Hill. This seismicity follows a similar trend to the Belham Valley Fault and proposed dyke orientations for the region (Hautmann et al., 2009; Mattioli et al., 1998). Finally, the NE cluster is more compact, with hypocenters not showing an increase in depth to the NE as was previously seen with original MVO hypocenters.

4.1 NE Cluster

Aspinall et al. (1998) had proposed a migration in seismicity towards Soufrière Hills from Long Ground in the NE from 5 to 6 August. However, Roman et al. (2008) proposed that the horizontal error was larger than the radius of the cluster, and hence no migration could be justified. Our calculated hypocenters show earthquakes early in the sequence to be located near Long Ground at depths of 1–4 km bsl (Figure 5)—associated errors for

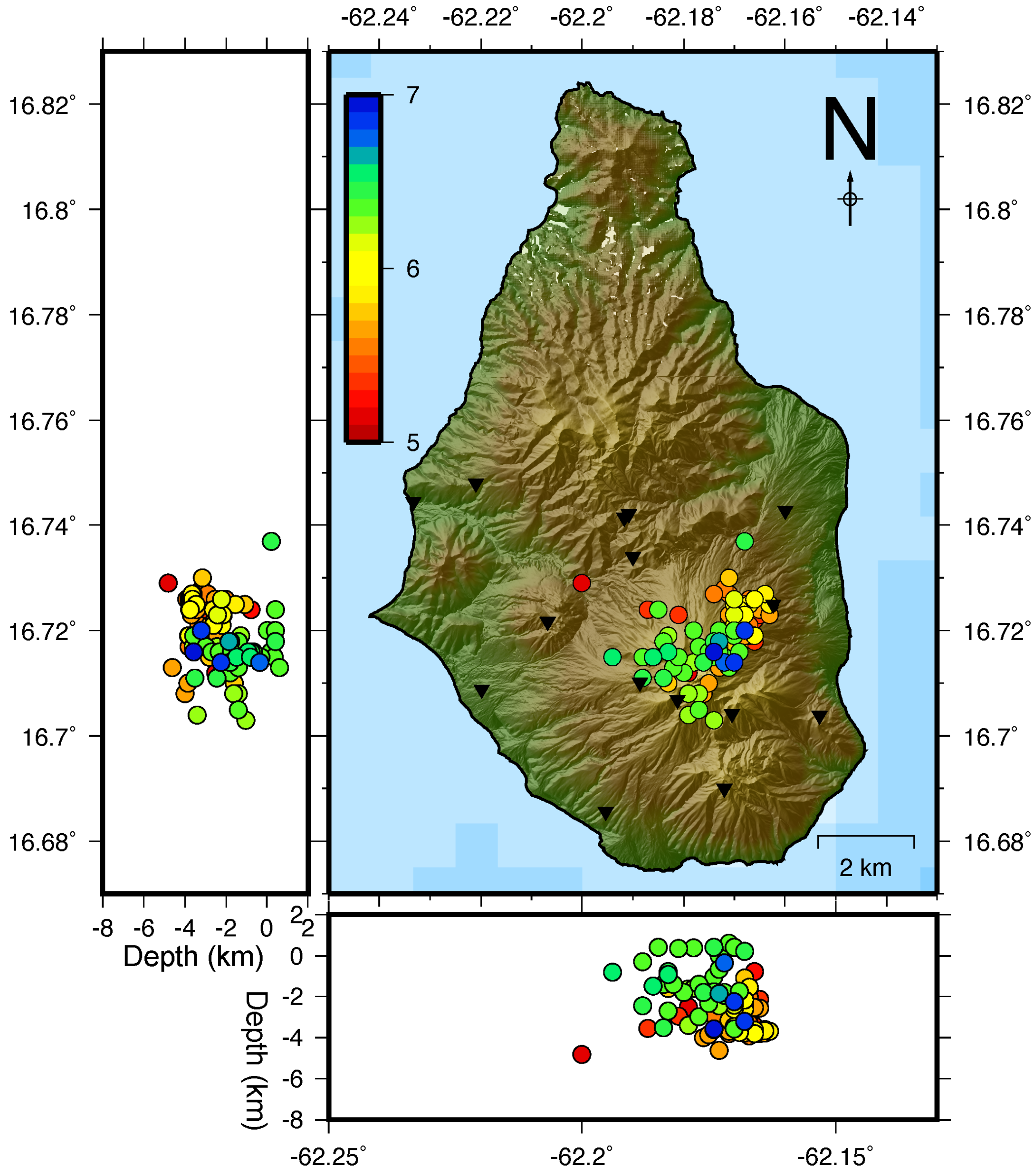

Figure 5 Earthquake hypocenters from 5 to 6 August 1995 coloured by time for all high-quality events.

the earthquakes are shown in Figure S14A. On 6 August, earthquakes migrated SW towards the flanks of Soufrière Hills. Using the filtered high-quality events, we confirm a migration of seismicity towards Soufrière Hills Volcano over a two-day period from Long Ground. However, even though our results agree with the interpretation from Aspinall et al. (1998) that the seismicity migrated, we found that the distance of migration was far more restricted than was originally postulated.

4.2 SGH Cluster

Prior to the Soufrière Hills eruption in 1995, 30-year cyclic episodes of earthquake swarms were recorded in southern Montserrat, mostly beneath the main summit (Shepherd et al., 1971; Young et al., 1998). However, it is thought that distal seismicity was recorded beneath St George's Hill in 1933–1937, although these use poorly constrained hypocenters that carry large uncertainties (Powell, 1938). This suggests that St George's Hill could have been seismically active in previous unrest episodes. No seismicity was recorded beneath St George's Hill in the years leading up to the eruption in 1995, and there is little evidence for a volcanic system in that area (Harford et al., 2002). Hypocenters by Aspinall et al. (1998) were located at depths of 4–6 km bsl, and relocated hypocenters by Miller et al. (2010) highlighted seismicity located at 3.5 km WNW of Soufrière Hills and at depths of 3–4 km. The focal mechanisms during this period show a mixture of normal faulting with WNW-ESE extension and NE-SW extension (Miller et al., 2010). Our locations, when using high quality hypocenters, show events located 3–4 km NW of Soufrière Hills at depth range of 1–5 km. Over half of the earthquakes during this time period are located between a depth of 3.5–5.2 km showing a wider range in depth location than found by Miller et al. (2010).

Our hypocenters show a connection between the NW flank of Soufrière Hills and St George's Hill that was not

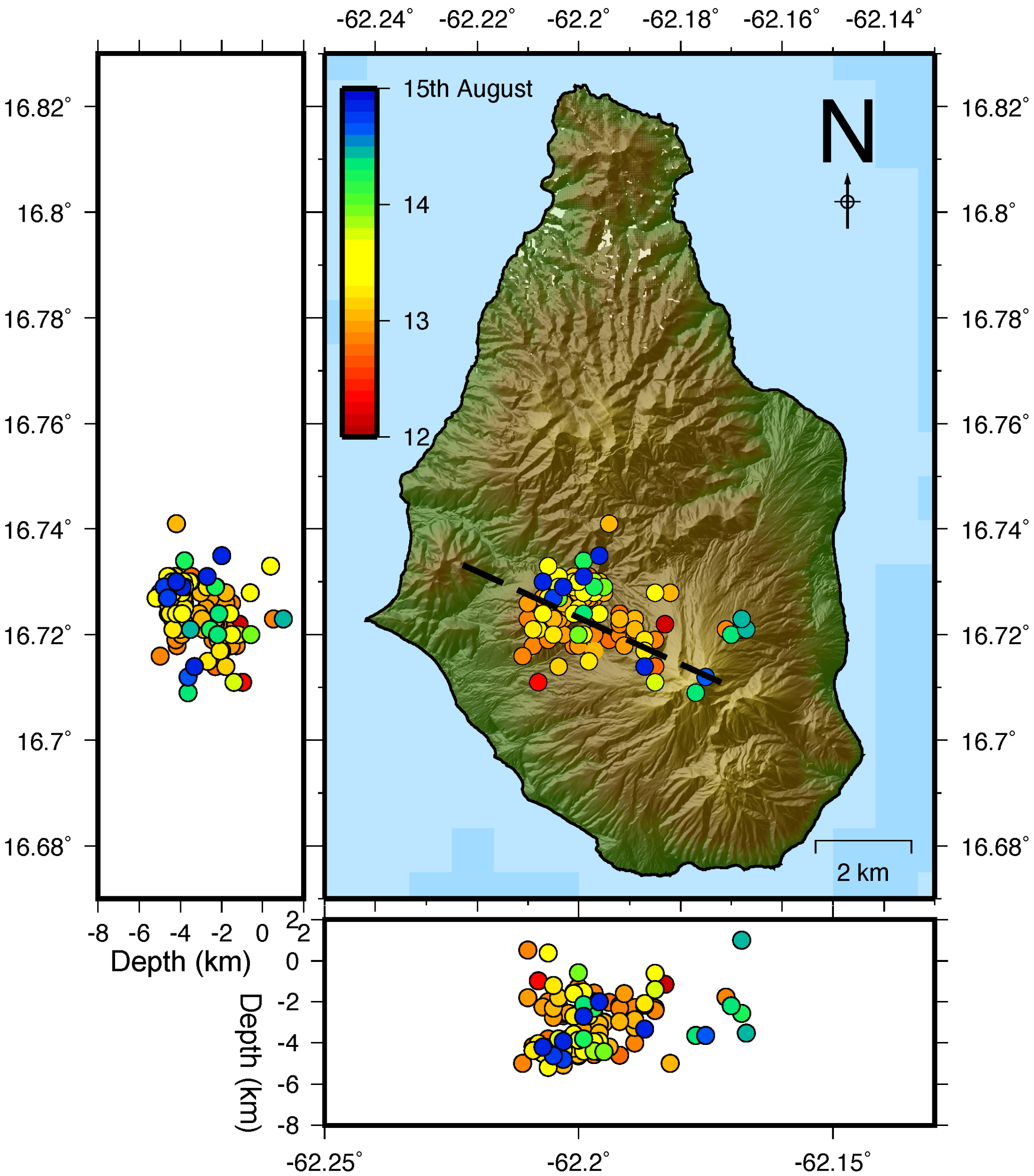

Figure 6 Diagram showing high-quality hypocenters from 11 to 14 August 1995. Hypocenters are coloured by time. Black line represents suggested dyke projection.

previously seen with the MVO hypocenters (Hypocentral errors of this cluster are shown in Figure S14B). Seismicity is recorded on the flanks of Soufrière Hills towards the end of 12 August, before the majority of seismicity is recorded beneath St George's Hill thereafter. Hypocenters are coloured by time to help highlight any migration of seismicity during this three day period (Figure 6). We note that there is no clear migration of seismicity when using the high quality hypocenters, but we propose that this lineation is representative of a feature that would benefit from further analysis such as joint relocation.

Volcano-tectonic earthquakes can be triggered on regionally aligned faults by low internal pressures produced by an intruding magmatic body (Vargas-Bracamontes and Neuberg, 2012). This could be a plausible reason for the seismicity recorded during the SGH cluster that follows similar trends to the Belham Valley Fault and the Richmond Hill Faults. White and McCausland (2016) originally proposed that this distal cluster was a result of the local stress field triggering seismicity along faults. Our relocated hypocenters show a clear lineation of seismicity to the WNW with a slight migration of hypocenters through time, possibly representing dyke migration during this period. There is a separate geothermal system beneath St George's Hill, evidenced by increased well temperatures and increased seismic velocities (Ryan et al., 2013). St George's Hill is located at an intersection of two fault systems; this produces zones of crustal weakness that can act as preferential paths for magmatic intrusions (Ryan et al., 2013; Faulds et al., 2011). Therefore, a possible scenario for this distal seismicity could be dyke propagation in this region, that was stalled beneath St George's Hill. However, it can not be ruled out that seismicity was triggered by changes in local stress fields activating localised faults as suggested by White and McCausland (2016).

Following the main trend in seismicity during this time period, we propose a WNW dyke orientation, shown in Figure 6. Our proposed dyke follows similar trends found by Baird et al. (2015), Hautmann et al. (2009) and Mattioli et al. (1998), who suggested a dyke orientation varying from NW to WNW. This also follows the trend in volcanic complexes recorded at Soufrière Hills and the Belham Valley Fault which extends towards St George's Hill (Figure 1).

Our different dyke orientation highlights the difference in interpretation during this timeframe when using different location methodologies and the implications for hazard assessment. Our new proposed location method for Montserrat is shown to reduce location errors and have a higher percentage of trusted hypocenters, supporting confidence in outputted locations and interpretations. This distal cluster would benefit from further analysis such as joint location methods which would further refine the seismicity, allowing estimation rates for dyke propagation, and if the seismicity was related to pre-existing faults.

4.3 Implications for Models of the Magmatic System

Previous research revealed conflicting results to proposed dyke projections across Montserrat, displayed in Figure 7. Regional stress and the orientation of mapped dykes on Montserrat are characterised by a NE-SW arc-normal compression (Wadge, 1986; Bonneton and Scheidegger, 1981). This coincides with NNW trending faults across the Soufrière Hills complex and fits with other larger faults in the region, such as the Belham Valley Fault, Richmond Hills Fault, and the Montserrat-Havers Fault Zone (which extends offshore from southern Montserrat towards Guadeloupe (Feuillet et al., 2010)). Domes from the Soufrière Hills complex are aligned similar to the strike of faults in the region (Figure 1), suggesting that these formed as a result of a NNE-SSW crustal extension, such as a NNW trending dyke (Baird et al., 2015).

A NNW-SSE dyke was proposed by Hautmann et al. (2009) and Mattioli et al. (1998), who used finite element modelling and GPS data from the early stages of the eruption. Shear Wave Splitting measurements from 1996 to 2007 show regions to have a WNW strike suggesting anisotropy is structurally controlled and fits a NNW orientation (Baird et al., 2015). Neuberg et al. (2022) showed that GPS observations are best explained by a dual source model of a shallow deflating source and deeper inflating source with azimuths of 293° and 263° respectively. Roman et al. (2006, 2008) proposed a NE trending dyke based on trends in P axes from Volcano-Tectonic (VT) seismicity. 90 degree rotations in P axes have been observed throughout the eruption, coinciding with periods of increased magma extrusions (Roman et al., 2006); these require pressures higher than regional stresses and are thought to relate to an inflating magmatic system (Vargas-Bracamontes and Neuberg, 2012). Analysis of seismic anisotropy from 1996–2007 suggested a NE-orientated dyke was more likely during this time period (Roman et al., 2011). A NNE oriented dyke was also proposed by Miller et al. (2010) using 1995 seismic data, and a NE orientation by Chardot et al. (2010) using strain measurements in 2008; however, both studies suggested these were short lived trends.

P axes parallel to the regional compressive stress (in this case NE-SW) have been shown to occur for VT seismicity at the tips of propagating dykes (Ukawa and Tsukahara, 1996) and for VT earthquakes occurring on shear planes extending obliquely from the edge on an inflating dyke (Hill, 1977). Time periods where NE-SW dyke orientations were proposed were seen underneath St George's Hill, Windy Hill and Soufrière Hills (Miller et al., 2010). These fit with time frames where we see the possibility for migration of seismicity in this region, such as the SGH cluster. Hence, an alternative interpretation for the presence of earthquakes with rotated P-axes is the propagation of an intruding dyke, instead of a different dyke orientation.

A WNW trend in dyke orientation fits with geological evidence, other mapped dykes and fault complexes across the island (Feuillet et al., 2010); the evidence from our analysis shows a strong basis for a dyke of this orientation during this time period. Seismicity recorded during the NE cluster shows a migration in seismicity to the SW from Long Ground, suggesting a NE orientation. However, as proposed by Miller et al. (2010) it is likely that these are short lived trends, which could be the activation of faults in the region due to magmatic intrusion, triggering distal clusters as proposed by White and McCausland (2016). This could also explain seismicity recorded beneath Windy Hill during the early stages of the eruption.

Our relocations suggest that seismicity during the SGH cluster could also be interpreted as dyke propagation over a two day period ending beneath St George's Hill. Using this seismicity cluster, we suggest that the main dyke orientation responsible for the Soufrière Hills eruption was a WNW orientated dyke, fitting with interpretations by Baird et al. (2015); Hautmann et al. (2009) and Mattioli et al. (1998) and the direction of local faults and volcanic complexes. Seismicity to the NE is interpreted as a short lived trend resulting from an increase in magmatic pressure beneath Soufrière Hills during the early stages of the eruption, supporting previous work by Miller et al. (2010). Our refined relocations for the NE cluster confirm the migration of seismicity towards Soufrière Hills that was previously suggested by Aspinall et al. (1998) but discounted due to large hypocenter errors. This highlights how testing different location methodologies can be a vital step in reducing location errors and improving hypocenters.

We provide a robust method for improving earthquake locations in real-time, without computer-intensive methods needed for further analysis. Additional research using alternative methods such as joint-location methods would likely improve calculated hypocenters, but is not always possible for observatories during increased unrest. Our suggested method highlights how hypocenters can be improved for real-time monitoring, vital for hazard monitoring at observatories which may have time and computing

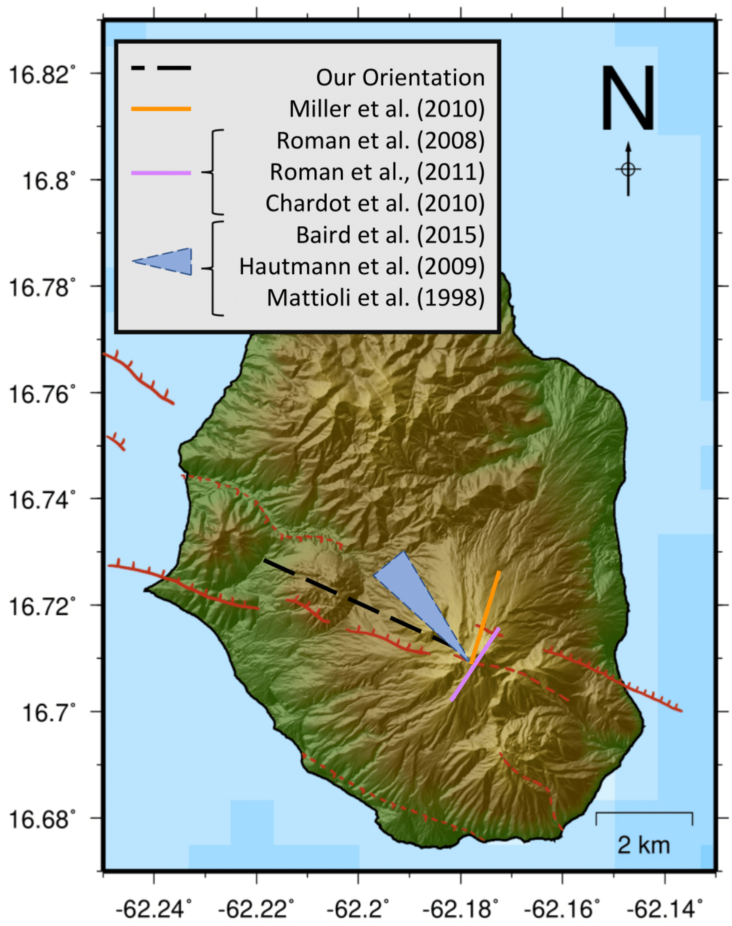

Figure 7 Our proposed dyke orientation (black dashed line) with previously suggested dyke orientations. Red lines represent local faults on Montserrat.

constraints.

5 Conclusions

Testing of MVO's current setup for earthquake location on Montserrat suggested an alternative location setup was more suitable. Synthetic earthquakes were used to compare four velocity models and location methods to determine which setup was optimal for locating earthquakes on Montserrat. Comparison with MVO's current setup suggested an alternative location algorithm and velocity model was more suited for locating earthquakes and resulted in an increased number of trusted hypocenters. Relocations using this optimal setup focussed on four distal clusters from July–November 1995 which had been previously identified by Aspinall et al. (1998) and Miller et al. (2010).

The NE cluster showed a migration of seismicity towards Soufrière Hills, which had previously been noted by Aspinall et al. (1998) but discounted by Roman et al. (2008) due to the horizontal errors being larger than the radius of the cluster. Our improved hypocenters cover a migration distance larger than the calculated errors and agree with Aspinall et al. (1998) locations during this time period.

A distal cluster under St George's Hill was previously thought to be a result of stress changes from a magmatic intrusion under Soufrière Hills Volcano, triggering pre-existing fault structures or disturbing the local hydrothermal system (Aspinall et al., 1998; Miller et al., 2010; White and McCausland, 2016). However, our locations show a temporal trend in seismicity with hypocenters migrating from the flanks of Soufrière Hills Volcano towards St George's Hill over a two-day period. An alternative interpretation of this seismicity cluster could be a propagating dyke towards St George's Hill. As such, our proposed WNW dyke orientation would be consistent with previously proposed dyke orientations over the course of the recent eruption.

Contrasting interpretations of seismicity demonstrate the importance of testing the method used for locating earthquakes and indicates this should be applied at systems elsewhere. It is important to understand how the location method and models that are currently being used operate and how well they perform at locating earthquakes in each region. It is important to understand if the calculated errors represent the actual accuracy of the hypocenters and if there is an alternative location method or velocity model which may be more suited for that environment. It is possible that several observatories are using outdated methodologies, and improvements to the location methods and catalogues would result in additional understanding of the volcanic systems in the region without the need for further computational analysis or deployment of seismic arrays.

Acknowledgements

We would like to thank the Montserrat Volcano Observatory for providing the seismic data used in this paper; this was provided under a data agreement between J.E. and MVO. We would also like to thank the reviewers on each stage of this paper submission and William Frank for his support during the final stages which included suggestions that were integral to the completion of this paper.

J.E. was funded by NERC studentship NE/L002582/1. J.E. is currently funded by a Marie Curie Fellowship Grant.

Data and code availability

The seismic catalogue used in this paper was provided by the Montserrat Volcano Observatory through a data agreement between J.E. and MVO. Data requests should be made to the Montserrat Volcano Observatory. Code used for real and synthetic hypocenter calculations was from the location methods Hypocenter and NonLinLoc. The Hypocenter program was used within the SEISAN software package which can be downloaded at: https://www.geo.uib.no/seismo/SOFTWARE/SEISAN/. The NonLinLoc software can be downloaded online at: http://alomax.free.fr/nlloc/index.html.

The supplemental material provides additional images relating to the velocity models, seismic stations and synthetic earthquake grid used for the synthetic testing. It includes a more comprehensive table of results from the synthetic testing and a full list of earthquake hypocenters and corresponding errors for events used in this analysis.

Competing interests

The authors declare no competing interests.

References

Aspinall, W., Miller, A., Lynch, L., Latchman, J., Stewart, R., White, R., and Power, J. Soufrière Hills eruption, Montserrat, 1995–1997: Volcanic earthquake locations and fault plane solutions. *Geophysical Research Letters*, 25(18):3397–3400, 1998. doi: 10.1029/98GL00858.

Baird, A. F., Kendall, J.-M., Sparks, R. S. J., and Baptie, B. Transtensional deformation of Montserrat revealed by shear wave splitting. *Earth and Planetary Science Letters*, 425:179–186, 2015. doi: 10.1016/j.epsl.2015.06.006.

Bird, P. An updated digital model of plate boundaries. *Geochemistry, Geophysics, Geosystems*, 4(3), 2003. doi: 10.1029/2001GC000252.

Bonneton, J.-R. and Scheidegger, A. Relations between fracture patterns, seismicity and plate motions in the Lesser Antilles. *Journal of Structural Geology*, 3(4):359–369, 1981. doi: 10.1016/0191-8141(81)90036-5.

Bono, A., Lauciani, V., Margheriti, L., and Quintiliani, M. Caravel: A New Earthworm-Based Open-Source Development for the Italian Seismic Monitoring System. *Seismological Research Letters*, 92(3):1738–1746, 2021. doi: 10.1785/0220200355.

Bratt, S. and Nagy, W., . The LocSAT Program. *Science Applications International Corporation, San Diego*, 1991.

Chardot, L., Voight, B., Foroozan, R., Sacks, S., Linde, A., Stewart, R., Hidayat, D., Clarke, A., Elsworth, D., Fournier, N., et al. Explosion dynamics from strainmeter and microbarometer observations, Soufrière Hills Volcano, Montserrat: 2008–2009. *Geophysical Research Letters*, 37(19), 2010.

Dunn, O. Multiple comparisons using rank sums. *Technometrics*, 6:241–252, 1964. doi: 10.1080/00401706.1964.10490181.

Faulds, J. E., Hinz, N. H., Coolbaugh, M. F., Cashman, P. H., Kratt, C., Dering, G., Edwards, J., Mayhew, B., and McLachlan, H. Assessment of favorable structural settings of geothermal systems in the Great Basin, western USA. *Geothermal Resources Council Transactions*, 35:777–783, 2011.

Feuillet, N., Leclerc, F., Tapponnier, P., Beauducel, F., Boudon, G., Le Friant, A., Deplus, C., Lebrun, J.-F., Nercessian, A., Saurel, J.-M., et al. Active faulting induced by slip partitioning in Montserrat and link with volcanic activity: New insights from the 2009 GWADASEIS marine cruise data. *Geophysical Research Letters*, 37(19), 2010. doi: 10.1029/2010GL042556.

Harford, C., Pringle, M., Sparks, R., and Young, S. The volcanic evolution of Montserrat using 40Ar/39Ar geochronology. *Geological Society, London, Memoirs*, 21(1):93–113, 2002. doi: 10.1144/GSL.MEM.2002.021.01.05.

Hautmann, S., Gottsmann, J., Sparks, R. S. J., Costa, A., Melnik, O., and Voight, B. Modelling ground deformation caused by oscillating overpressure in a dyke conduit at Soufrière Hills Volcano, Montserrat. *Tectonophysics*, 471(1-2):87–95, 2009. doi: 10.1016/j.tecto.2008.10.021.

Hill, D. P. A model for earthquake swarms. *Journal of Geophysical Research*, 82(8):1347–1352, 1977. doi: 10.1029/JB082i008p01347.

Hobro, J. W., Singh, S. C., and Minshull, T. A. Three-dimensional tomographic inversion of combined reflection and refraction seismic traveltime data. *Geophysical Journal International*, 152(1): 79–93, 2003. doi: 10.1046/j.1365-246X.2003.01822.x.

Johnson, C. E., Bittenbinder, A., Bogaert, B., Dietz, L., and Kohler, W. Earthworm: A flexible approach to seismic network processing. *Iris newsletter*, 14(2):1–4, 1995.

Klein, F. *User's guide to HYPOINVERSE-2000: A Fortran program to solve for earthquake locations and magnitudes*. US Geological Survey Open File Rept. 02-171, 2002. doi: 10.3133/ofr02171.

Lienert, B. R., Berg, E., and Frazer, L. N. HYPOCENTER: An earthquake location method using centered, scaled, and adaptively damped least squares. *Bulletin of the Seismological Society of America*, 76(3):771–783, 1986. doi: 10.1785/BSSA0760030771.

Lomax, A. NonLinLoc Home Page, 2001.

Mattioli, G. S., Dixon, T. H., Farina, F., Howell, E. S., Jansma, P. E., and Smith, A. L. GPS measurement of surface deformation around Soufrière Hills volcano, Montserrat from October 1995 to July 1996. *Geophysical Research Letters*, 25(18):3417–3420, 1998. doi: 10.1029/98GL00931.

Miller, V., Voight, B., Ammon, C. J., Shalev, E., and Thompson, G. Seismic expression of magma-induced crustal strains and localized fluid pressures during initial eruptive stages, Soufrière Hills Volcano, Montserrat. *Geophysical Research Letters*, 37(19), 2010. doi: 10.1029/2010GL043997.

Miller, V. L. *Crustal Response to Changes in the Magmatic System at the Soufrière Hills Volcano, Montserrat*. PhD thesis, Pennslyvania

State University, 2011.

MVO. MVO OFR 23/02. *MVO Open File Rep*, 2023.

Neuberg, J., Taisne, B., Burton, M., Ryan, G., Calder, E., Fournier, N., and Collinson, A. A review of tectonic, elastic and visco-elastic models exploring the deformation patterns throughout the eruption of Soufrière Hills volcano on Montserrat, West Indies. *Journal of Volcanology and Geothermal Research*, 425: 107518, 2022. doi: 10.1016/j.jvolgeores.2022.107518.

Paulatto, M., Annen, C., Henstock, T. J., Kiddle, E., Minshull, T. A., Sparks, R., and Voight, B. Magma chamber properties from integrated seismic tomography and thermal modeling at Montserrat. *Geochemistry, Geophysics, Geosystems*, 13(1), 2012. doi: 10.1029/2011GC003892.

Podvin, P. and Lecomte, I. Finite difference computation of traveltimes in very contrasted velocity models: a massively parallel approach and its associated tools. *Geophysical Journal International*, 105(1):271–284, 1991. doi: 10.1111/j.1365-246X.1991.tb03461.x.

Powell, C. The Royal Society expedition to Montserrat, BWI final report. *Phil. Trans. R. Soc. Lond. A*, 237(771):1–34, 1938. doi: 10.1098/rsta.1938.0002.

Power, J. A., Wyss, M., and Latchman, J. L. Spatial variations in the frequency-magnitude distribution of earthquakes at Soufrière Hills Volcano, Montserrat, West Indies. *Geophysical Research Letters*, 25(19):3653–3656, 1998. doi: 10.1029/98GL00430.

Richards, P.G., F. W. D. S. and W-Y, K. The Applicability of Modern Methods of Earthquake Location. *Pure Applied Geophysics*, 163: 351–372, 2006. doi: 10.1007/s00024-005-0019-5.

Roman, D., Neuberg, J., and Luckett, R. Assessing the likelihood of volcanic eruption through analysis of volcanotectonic earthquake fault–plane solutions. *Earth and Planetary Science Letters*, 248(1-2):244–252, 2006. doi: 10.1016/j.epsl.2006.05.029.

Roman, D., De Angelis, S., Latchman, J., and White, R. Patterns of volcanotectonic seismicity and stress during the ongoing eruption of the Soufrière Hills Volcano, Montserrat (1995–2007). *Journal of Volcanology and Geothermal Research*, 173(3-4): 230–244, 2008. doi: 10.1016/j.jvolgeores.2008.01.014.

Roman, D. C., Savage, M. K., Arnold, R., Latchman, J. L., and De Angelis, S. Analysis and forward modeling of seismic anisotropy during the ongoing eruption of the Soufrière Hills Volcano, Montserrat, 1996–2007. *Journal of Geophysical Research: Solid Earth*, 116(B3), 2011. doi: 10.1029/2010JB007667.

Rowe, C., Thurber, C., and White, R. Dome growth behavior at Soufrière Hills Volcano, Montserrat, revealed by relocation of volcanic event swarms, 1995–1996. *Journal of Volcanology and Geothermal Research*, 134(3):199–221, 2004. doi: 10.1016/j.jvolgeores.2004.01.008.

Ryan, G., Peacock, J., Shalev, E., and Rugis, J. Montserrat geothermal system: A 3D conceptual model. *Geophysical Research Letters*, 40(10):2038–2043, 2013. doi: 10.1002/grl.50489.

Shalev, E. and Lees, J. M. Cubic B-splines tomography at Loma Prieta. *Bulletin of the Seismological Society of America*, 88(1): 256–269, 1998. doi: 10.1785/BSSA0880010256.

Shalev, E., Kenedi, C., Malin, P., Voight, V., Miller, V., Hidayat, D., Sparks, R., Minshull, T., Paulatto, M., Brown, L., et al. Three-dimensional seismic velocity tomography of Montserrat from the SEA-CALIPSO offshore/onshore experiment. *Geophysical Research Letters*, 37(19), 2010. doi: 10.1029/2010GL042498.

Shepherd, J., Tomblin, J., and Woo, D. Volcano-seismic crisis in Montserrat, West Indies, 1966–67. *Bulletin volcanologique*, 35 (1):143–162, 1971. doi: 10.1007/BF02596813.

Ukawa, M. and Tsukahara, H. Earthquake swarms and dike intrusions off the east coast of Izu Peninsula, central Japan. *Tectonophysics*, 253(3):285–303, 1996. doi: 10.1016/0040-1951(95)00077-1.

Vargas-Bracamontes, D. and Neuberg, J. Interaction between regional and magma-induced stresses and their impact on volcano-tectonic seismicity. *Journal of volcanology and geothermal research*, 243:91–96, 2012. doi: 10.1016/j.jvolgeores.2012.06.025.

Wadge, G. The dykes and structural setting of the volcanic front in the Lesser Antilles island arc. *Bulletin of Volcanology*, 48(6): 349–372, 1986. doi: 10.1007/BF01074466.

Waldhauser, F. hypoDD–A program to compute double-difference hypocenter locations. Technical report, Earthquake Science Center, 2001.

White, R. and McCausland, W. Volcano-tectonic earthquakes: A new tool for estimating intrusive volumes and forecasting eruptions. *Journal of Volcanology and Geothermal Research*, 309: 139–155, 2016. doi: 10.1016/j.jvolgeores.2015.10.020.

Young, S. R., Francis, P. W., Barclay, J., Casadevall, T., Gardner, C., Darroux, B., Davies, M., Delmelle, P., Norton, G., Maciejewski, A., et al. Monitoring SO_2 emission at the Soufrière Hills Volcano: Implications for changes in eruptive conditions. *Geophysical Research Letters*, 25(19):3681–3684, 1998. doi: 10.1029/98GL01406.